

RESEARCH PAPER

Preclinical evaluation of a monoclonal antibody targeting the epidermal growth factor receptor as a radioimmunodiagnostic and radioimmunotherapeutic agent

GL Ray¹, KE Baidoo¹, KJ Wong², M Williams², K Garmestani¹, MW Brechbiel¹ and DE Milenic¹¹Radioimmune & Inorganic Chemistry Section, Radiation Oncology Branch, Center for Cancer Research, National Cancer Institute, National Institutes of Health, Bethesda, MD, USA, and ²Molecular Imaging Program, Center for Cancer Research, National Cancer Institute, National Institutes of Health, Bethesda, MD, USA

Background and purpose: The studies described here are the first to evaluate the *in vitro* and *in vivo* properties of ¹¹¹In-CHX-A''-panitumumab for radioimmunotherapy (α - and β -emitters) and radioimmunodiagnosis (single photon emission computed tomography and positron emission tomography).

Experimental approach: Twenty-seven human carcinoma cell lines were analysed for expression of epidermal growth factor receptors by flow cytometry. Panitumumab was conjugated with CHX-A''-DTPA (diethylenetriamine-pentaacetic acid) and radiolabelled with ¹¹¹In. Immunoreactivity of the CHX-A''-DTPA-panitumumab and ¹¹¹In-CHX-A''-DTPA-panitumumab was evaluated by radioimmunoassays. Tumour targeting was determined *in vivo* by direct quantitation of tumour and normal tissues and by γ -scintigraphy.

Key results: For 26 of 27 human tumour cell lines, 95% of the cells expressed epidermal growth factor receptors over a range of intensity. Immunoreactivity of panitumumab was retained after modification with CHX-A''-DTPA. Radiolabelling of the immunoconjugate with ¹¹¹In was efficient with a specific activity of 19.5 ± 8.9 mCi·mg⁻¹ obtained. Immunoreactivity and specificity of binding of the ¹¹¹In-panitumumab was shown with A431 cells. Tumour targeting by ¹¹¹In-panitumumab was demonstrated in athymic mice bearing A431, HT-29, LS-174T, SHAW or SKOV-3 s.c. xenografts with little uptake observed in normal tissues. The ¹¹¹In-panitumumab was also evaluated in non-tumour-bearing mice. Pharmacokinetic studies compared the plasma retention time of the ¹¹¹In-panitumumab in both non-tumour-bearing and A431 tumour-bearing mice. Tumour targeting was also visualized by γ -scintigraphy.

Conclusions and implications: Panitumumab can be efficiently radiolabelled with ¹¹¹In with high labelling yields. Based on the efficiency in tumour targeting and low normal tissue uptake, panitumumab may be an effective targeting component for radioimmunodiagnostic and radioimmunotherapeutic applications.

British Journal of Pharmacology (2009) **157**, 1541–1548; doi:10.1111/j.1476-5381.2009.00327.x

Keywords: panitumumab; radioimmunodiagnosis; radioimmunotherapy; EGFR; preclinical evaluation; ¹¹¹In

Abbreviations: %ID·g⁻¹, percentage of injected dose per gram; %ID·mL⁻¹, percentage of injected dose per millilitre; BSA, bovine serum albumin; DMEM, Dulbecco's modified Eagle's medium; DTPA, diethylenetriamine-pentaacetic acid; EGFR, epidermal growth factor receptor; FDA, Food and Drug Administration; IgG, immunoglobulin; mAb, monoclonal antibody; PBS, phosphate-buffered saline

Introduction

The field of oncology continues to focus on novel targeted strategies designed to inhibit specific cancer pathways and

key molecules responsible for tumour growth and progression. More than two decades after their introduction, monoclonal antibody (mAb)-targeted therapies have generally become recognized as significantly influencing cancer therapy. Because they can selectively target a cytotoxic agent, mAb 'magic bullets' have the potential to increase the therapeutic index (benefit vs. risk) (Milenic *et al.*, 2004a). For example, radioimmunoconjugates (RICs), such as Zevalin™ and Bexxar™ have been highly efficacious for treating

Correspondence: Diane E Milenic, National Institutes of Health, 10 Center Drive, MSC-1088, Building 10, Room 1B40, Bethesda, MD 20892, USA. E-mail: dm71q@nih.gov

Received 26 March 2009; accepted 31 March 2009

lymphoma (Knox *et al.*, 1996; Vose *et al.*, 2000). The targeted nature of such therapies offers the promise of greater efficacy and less toxicity (Milenic *et al.*, 2004a). These successes highlight the need for additional radioimmunotherapeutic agents.

The epidermal growth factor receptor (EGFR), a member of the ErbB family plays an essential role in normal organ development. EGFR functions as an initiation point of various intracellular signalling cascades that mediate morphogenesis and differentiation (Salomon *et al.*, 1995; Wells, 1999; Baselga, 2002). Overexpression or mutation of the receptor can lead to increased cellular proliferation, apoptosis, angiogenesis, tumour invasiveness and metastases; properties commonly associated with cancer cells (Salomon *et al.*, 1995; Baselga, 2002). Blockade of this receptor is a major strategy for the development of cancer therapeutics.

Panitumumab (Vectibix, Amgen, CA, USA), a fully human mAb that binds the EGFR with high affinity, is approved by the Food and Drug Administration (FDA) for the treatment of patients with EGFR-expressing, metastatic colorectal carcinoma with disease progression on or following fluoropyrimidine-, oxiplatin- and irinotecan-containing chemotherapy regimens (Yang *et al.*, 1999; Giusti *et al.*, 2007). Panitumumab monotherapy is well tolerated and has been successful in slowing disease progression and improving progression-free survival (Cohenuram and Saif, 2007; Giusti *et al.*, 2007). It is conceivable that radiolabelled formulations of panitumumab would have applications for non-invasive imaging in order to characterize EGFR-positive tumours biochemically and thus to select patient populations that could benefit from therapy, as well as direct therapy of the tumours when used as a radioimmunotherapeutic agent. This study assesses the potential of panitumumab as a RIC, both *in vitro* and *in vivo*, using ¹¹¹In-labelled panitumumab. This evaluation includes tumour targeting of the RIC in five tumour xenograft models using γ -scintigraphic imaging combined with direct analysis of both tumour and normal tissues.

Methods

Cell lines

Growth conditions for the human carcinoma cell lines A375, A431, BxPC3, CBS, DLD-1, DU145, GEO, HT-29, KM12SM (a gift from Dr. St. Croix, NCI), LNCaP, LS-174T, M21, MB-MDA-231, MCF-7, N87, PC3, SHAW (provided by Dr. Mitchell, NCI), MIP, WiDr, SKOV-3 and 22Rv1 (see Table 1 for the tumour type) have been previously detailed (Greiner, 1986; Guadagni *et al.*, 1990; Garmestani *et al.*, 2002; Milenic *et al.*, 2005; Boswell *et al.*, 2008; Milenic *et al.*, 2008; Regino *et al.*, 2009). The ACHN cells were grown in Dulbecco's modified Eagle's medium (DMEM) with sodium pyruvate (1 mM) and sodium bicarbonate (NaHCO₃; 1.5 g·L⁻¹). SK-MEL and U-87 MG were maintained in DMEM with glutamine and sodium pyruvate. OVCAR-3 and A549 were grown in RPMI-1640; A549 also required sodium pyruvate and glutamine. MiaPaCa-2 was maintained in DMEM containing glucose and NaHCO₃. The cells were maintained in a humidified incubator with 5% CO₂ at 37°C. All media contained 10% FetalPlex (Gemini Bio-Products, Woodland, CA, USA) and non-essential amino acids. Media and supplements were obtained from

Table 1 Flow cytometric analysis of epidermal growth factor receptor expression of and reactivity of panitumumab with human carcinoma cell lines

Tumour type	Cell line	Mean fluorescence intensity	% Positive cells
Breast	MCF-7	653.6	65.1
	MD-MBA-231	575.8	99.9
Colon	CBS	56.4	97.5
	DLD-1	138.9	99.9
	GEO	64.9	99.1
	HT-29	59.8	97.3
	KM12SM	78.9	95.6
	LS-174T	62.5	99.9
	MIP	167.3	98.9
Gastric	N87	46.1	97.8
Lung	A549	59.4	99.5
Melanoma	A-375	51.0	94.4
	M21	26.8	99.9
	SK-MEL	34.0	98.6
	OVCAR-3	433.6	99.9
Ovarian	SKOV-3	138.6	97.1
	BxPC3	191.8	99.9
Pancreatic	CFPAC-1	416.1	99.9
	MiaPaCa-2	421.3	99.2
	SHAW	118.5	99.9
	22Rv1	97.3	99.9
Prostate	DU145	330.2	99.9
	LNCaP	153.7	99.9
	PC3	150.9	99.9
	ACHN	253.6	99.9
Renal	A431	2072.2	99.3
Epidermoid	U-87 MG	75.1	99.9
Glioma			

Lonza (Walkersville, MD, USA) or Invitrogen (Carlsbad, CA, USA). Unless otherwise stated, all cell lines were obtained from ATCC (Manassas, VA, USA).

Flow cytometry

Epidermal growth factor receptor expression of the cell lines were evaluated by using standard flow cytometric techniques (Garmestani *et al.*, 2002; Milenic *et al.*, 2008). Cells were harvested and resuspended in phosphate-buffered saline (PBS; pH 7.2) containing 1% bovine serum albumin (BSA). Panitumumab (1 μ g; Amgen, Thousand Oaks, CA, USA) or HuIgG (ICN Pharmaceuticals, Inc., Costa Mesa, CA, USA) was added to the cells (1 \times 10⁶ per 100 μ L) and incubated at 4°C for 1 h. After washing with 1% BSA/PBS, the cells were incubated with Alexa Fluor488 Goat anti-human IgG (0.5 μ g per 100 μ L; Invitrogen) and incubated for 1 h at 4°C. The cells were washed, resuspended in 1 mL PBS and analysed using a FAC-SCalibur (10 000 events collected) with CellQuest software (BD Biosciences, San Jose, CA, USA).

mAb conjugation and radiolabelling

Panitumumab was conjugated with the bifunctional acyclic CHX-A''-DTPA (diethylenetriamine-pentaacetic acid) chelate by modification of established methods using a 10-fold molar excess of ligand to panitumumab (Wu *et al.*, 1997; Milenic *et al.*, 2008). The final concentration of the panitumumab was quantitated by the method of Lowry (Lowry *et al.*, 1951). The

number of ligand molecules conjugated to the mAb was assayed spectrophotometrically using the Y(III)–Arsenazo(III) complex (Pippin *et al.*, 1992).

Radio-iodination of panitumumab (50 µg) with Na¹²⁵I (0.5–1 mCi; PerkinElmer, Shelton, CT, USA) was performed by using Iodo-Gen (Pierce Chemical, Rockford, IL, USA). (Fraker and Speck, 1978; Milenic *et al.*, 2008). Radiolabelling of CHX-A''-panitumumab (50 µg) with ¹¹¹In (1–2 mCi) was performed as described by Garmestani *et al.* (2002). The radiolabelled products were purified with a PD-10 desalting column (GE Healthcare, Piscataway, NJ, USA) by using PBS as the eluent.

Radioimmunoassays

Immunoreactivity of the panitumumab-CHX-A''-DTPA conjugate was evaluated in a competition radioimmunoassay by using a modification of a previously reported method (Milenic *et al.*, 1991; Iwahashi *et al.*, 1999). EGFR (50 ng per 50 µL PBS; Sigma-Aldrich, St. Louis, MO, USA) was added to the wells of a 96-well plate. Following an overnight incubation at 4°C, the wells were treated with PBS/BSA. The solution was aspirated, and serial dilutions (0.01–1000 ng in 50 µL BSA/PBS) of unmodified panitumumab or panitumumab-CHX-A''-DTPA were then added to the wells in triplicate along with ¹²⁵I-panitumumab (~50 000 cpm per 50 µL BSA/PBS); one set of wells contained only BSA/PBS. The wells were washed after 4 h at 37°C; bound radioactivity was removed and counted in a γ-scintillation counter (Wizard One, PerkinElmer). The percentage of inhibition was calculated by using the control (no competitor) and plotted. HuM195, an anti-CD33 mAb (provided by Dr. McDevitt, Memorial Sloan Kettering Cancer Center), was used as a negative control.

Immunoreactivity of the ¹¹¹In-panitumumab was assessed in a radioimmunoassay as detailed previously. (Xu *et al.*, 2007; Milenic *et al.*, 2008). Serial dilutions of ¹¹¹In-panitumumab were added to methanol-fixed A431 cells (1 × 10⁶ per 50 µL PBS/BSA), incubated 2 h at 37°C, washed, pelleted, the supernatant decanted and the pellets counted in a γ-scintillation counter. The percentage of binding was calculated for each dilution and averaged. Specificity of the radiolabelled panitumumab was confirmed by adding unlabelled panitumumab (10 µg) to one set of tubes along with the radiolabelled panitumumab.

Tumour models and in vivo studies

All animal care and experimental protocols were approved by the National Cancer Institute Animal Care and Use Committee. The *in vivo* behaviour of the RIC was assessed by using non-tumour-bearing and A431, HT-29, LS-174T, SHAW and SKOV-3 tumour-bearing athymic mice (Charles River Laboratories, Wilmington, MA, USA). Four- to six-week-old female athymic mice received s.c. injections in the flank with 2–4 × 10⁶ cells in 0.2 mL of media containing 20% Matrigel™ (Becton Dickinson, Bedford, MA, USA). Animals were used for *in vivo* studies when the tumour diameter measured 0.4–0.6 cm.

Tumour targeting was quantitated by injecting mice (*n* = 5 per time point) i.v. via the tail vein with ¹¹¹In-CHX-A''-panitumumab (~7.5 µCi). The mice were killed at 24, 48, 72, 96 and 168 h by CO₂ inhalation. The blood, tumour and

major organs were collected, weighed and counted in a γ-scintillation counter. The percentage of injected dose per gram (%ID·g⁻¹) was determined for each tissue; the averages and standard deviations are presented.

Blood pharmacokinetics were performed with non-tumour-bearing mice (*n* = 5) and mice (*n* = 5) bearing A431 xenografts. ¹¹¹In-CHX-A''-Panitumumab (~7.5 µCi in 200 µL PBS) was administered by i.v. injection, blood samples (10 µL) were collected in heparinized capillary tubes, and the radioactivity measured in a γ-scintillation counter. The percentage of injected dose per millilitre (%ID·mL⁻¹) was calculated for each of the samples, and the average with the standard deviation plotted for each time point.

Radioimmunosciintigraphy was performed with A431, HT-29, LS-174T and SKOV-3 tumour-bearing mice to further validate ¹¹¹In-CHX-A''-panitumumab tumour targeting. Imaging studies were performed with s.c. tumour-bearing mice (*n* = 4–5) given i.v. injections of ¹¹¹In-CHX-A''-panitumumab (~100 µCi in 200 µL PBS). The mice were immobilized with 2.5% isoflurane (Abbott Laboratories, North Chicago, IL, USA) by using a Summit Anesthesia Solutions vaporizer (Bend, OR, USA) at a flow rate of ~1.0 L·min⁻¹. Images were acquired at 24, 48, 72 and 168 h with a large field of view (LFOV) γ-camera equipped with a pinhole collimator and a 20 c/c window centred on both photopeaks (173 and 247 KeV)²³. Approximately 100 000 counts were collected per image.

Results

The studies performed were designed to evaluate the *in vitro* and *in vivo* properties of ¹¹¹In-labelled panitumumab. Modification of panitumumab with the acyclic ligand CHX-A''-DTPA was performed at a 10:1 molar excess of chelate to protein yielding a final chelate to protein ratio of 1.6. The conjugation did not alter immunoreactivity of the mAb as determined by a competition radioimmunoassay (Figure 1). Radiolabel-

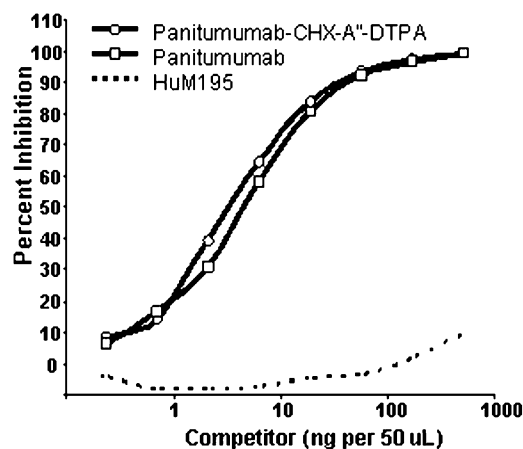


Figure 1 Evaluation of panitumumab immunoreactivity in a competition radioimmunoassay. The immunoreactivity of panitumumab-CHX-A''-DTPA (diethylenetriamine-pentaacetic acid) for purified epidermal growth factor receptor was compared with that of unmodified panitumumab. The anti-CD33 monoclonal antibody, HuM195 was used as a non-specific control.

ling of the CHX-A''-panitumumab with ^{111}In was efficient ($68.7 \pm 12.3\%$), resulting in a specific activity of $19.5 \pm 8.9 \text{ mCi}\cdot\text{mg}^{-1}$. When the RIC was incubated with EGFR over-expressing A431 cells, $74 \pm 7.5\%$ of the radioactivity was bound. The addition of $10 \mu\text{g}$ of unlabelled panitumumab resulted in only $4.0 \pm 0.9\%$ of the radioactivity being bound to the cells, demonstrating specificity.

Epidermal growth factor receptor expression by and binding of panitumumab to a variety of cell lines was explored using flow cytometric analysis. The percentages of tumour cells positively stained with panitumumab are presented along with the intensity of staining in Table 1. For each cell line studied, with the exception of MCF-7 cells, the proportion of cells expressing EGFR was greater than 95%. The A431 cells were found to have the highest mean fluorescence intensity value (2072), indicating extremely high EGFR expression on a per cell basis. Five other cell lines, MiaPaCa-2, MD-MBA-231, DU145, CFPAC-1 and OVCAR-3 also had high EGFR expression. Moderate EGFR expression was detected in eight of the cell lines while six cell lines exhibited low expression. EGFR expression by the melanoma cell lines, M21 and SK-MEL, was negligible.

Results of pharmacokinetic studies in athymic mice bearing A431 xenografts are shown in Figure 2. The profile for the RIC in the A431 tumour-bearing mice was noticeably different from the profile in non-tumour-bearing mice. One hour after injection, 50% of the ^{111}In -panitumumab was found to have cleared from the blood in the non-tumour-bearing mice. One minute after injection, the blood $\% \text{ID}\cdot\text{mL}^{-1}$ was 39; at 1 h it was 19.5. The $\% \text{ID}\cdot\text{mL}^{-1}$ continued to decrease reaching a value of 11.0 after 6 h, and by 168 h it was 1.0. In contrast, the clearance profile obtained from mice bearing the A431 xenografts was prolonged. At the initial time point, the $\% \text{ID}\cdot\text{mL}^{-1}$ was 46 and after 1 h decreased to 39. Six hours after injection, the blood $\% \text{ID}\cdot\text{mL}^{-1}$ of the ^{111}In -panitumumab was 26, and at 168 h, the $\% \text{ID}\cdot\text{mL}^{-1}$ was 1.7. This difference in the blood pharmacokinetics of the ^{111}In -panitumumab in the presence and absence of a tumour xenograft is reflected in the calculated clearance rates. The $t_{1/2\alpha}$ and $t_{1/2\beta}$ for mice bearing the A431 tumour xenografts was 2.6 and 53.7 h, respectively, while for the mice without tumours these values shifted to 0.5 and 14.0 h respectively.

In order to quantitate tumour targeting and normal organ distribution of the RIC, biodistribution studies were performed by using non-tumour-bearing athymic mice and mice bearing A431 s.c. tumours. In the absence of the A431 tumour (Figure 3A), the RIC achieved the highest $\% \text{ID}\cdot\text{g}^{-1}$ in the salivary glands at 96 h, the gall bladder at 72 h, the liver at 24 h, and the lungs at 48 h. However, as illustrated in Figure 3B, the $\% \text{ID}\cdot\text{g}^{-1}$ was lower in each corresponding tissue and time point in the presence of the tumour. The maximum $\% \text{ID}\cdot\text{g}^{-1}$ for the A431 tumour was observed 96 h after injection. These results suggest positive *in vivo* tumour targeting for the ^{111}In -radiolabelled panitumumab with low uptake of the RIC agent by normal tissues. The potential of ^{111}In -panitumumab to target other tumours was also evaluated. Table 2 summarizes the biodistribution results with mice bearing s.c. xenografts of HT-29, LS-174T, SHAW and SKOV-3. In each of the tumour models evaluated, the ^{111}In -labelled panitumumab demonstrated positive tumour targeting. Throughout the 7 day

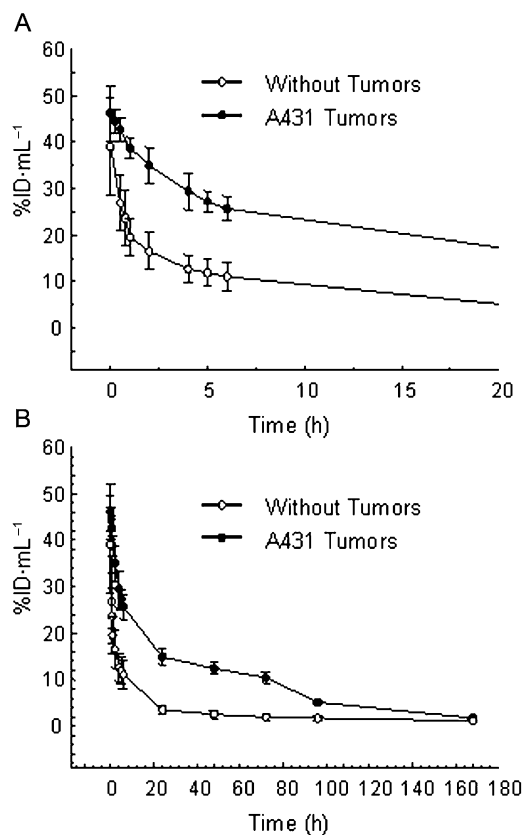


Figure 2 Blood pharmacokinetics of radiolabelled panitumumab. Mice ($n = 5$) bearing s.c. A431 xenografts as well as mice without tumours were given i.v. injections of ^{111}In -CHX-A''-panitumumab ($\sim 7.5 \mu\text{Ci}$) via the tail vein. Blood samples ($10 \mu\text{L}$) were collected over a 1 week period as described in *Methods*. The average $\% \text{ID}\cdot\text{mL}^{-1}$ (percentage of injected dose per millilitre) with the standard deviations is plotted. Panel A presents the first 20 h while Panel B presents the complete study period of 168 h.

study, the human colon carcinoma xenograft, LS-174T was observed to have the highest tumour uptake, reaching a maximum $\% \text{ID}\cdot\text{g}^{-1}$ of 44 at 48 h.

In general, a higher tumour $\% \text{ID}\cdot\text{g}^{-1}$ was obtained between 48 h and 96 h. The maximum $\% \text{ID}\cdot\text{g}^{-1}$ for the HT-29 was observed at 48 h, for the SHAW at 96 h and for SKOV-3 at 72 h. In general, the normal tissues of the tumour-bearing mice presented with a $\% \text{ID}\cdot\text{g}^{-1}$ of less than 8 for each tissue with the exception of the HT-29 tumour-bearing mice. In this instance, both the liver and spleen resulted in a high $\% \text{ID}\cdot\text{g}^{-1}$ of 16 at 72 h and 12 at 96 h respectively.

Radioimmunoscintigraphy was performed with mice bearing tumour xenografts to further demonstrate targeting by ^{111}In -panitumumab. Clear visualization of A431, HT-29, LS-174T and SKOV-3 xenografts were obtained by γ -scintigraphy. As expected for an intact radiolabelled antibody, a high uptake of the RIC in the blood pool (heart, lung and liver) was observed at 24 h, with subsequent clearance from the blood. Tumour targeting and decreasing background over the 1 week study period are illustrated in Figure 4 (top row). A similar pattern of tumour targeting and clearance was observed in the other tumour xenografts of which representative scintigraphs are presented (Figure 4, bottom row).

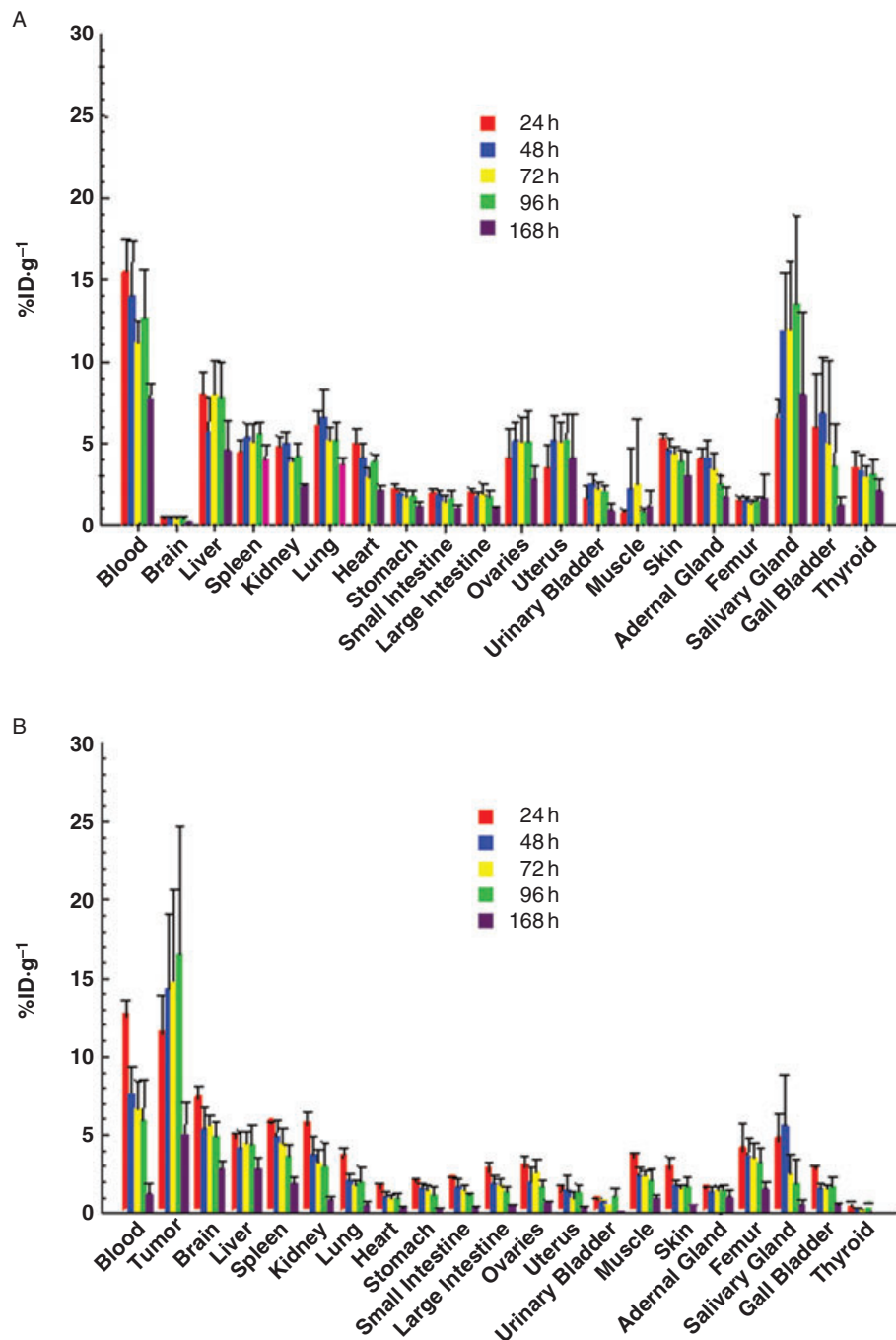


Figure 3 Biodistribution of ¹¹¹In-CHX-A''-panitumumab in tumour xenografts and normal tissues. Mice ($n = 5$) without tumour (Panel A) or bearing s.c. A431 xenografts (Panel B) were injected i.v. with ¹¹¹In-CHX-A''-panitumumab ($\sim 7.5 \mu\text{Ci}$). Mice were killed at the indicated times, when blood, tumour and tissues were removed, weighed and the radioactivity measured. The mean %ID.g⁻¹ (percentage of injected dose per gram) with standard deviations are plotted.

Discussion

The role of mutated or structurally altered EGFR in cellular transformation is well established (Mendelsohn and Baselga, 2006). Two mAbs that bind to the extracellular domain of EGFR, cetuximab and panitumumab have been approved by the FDA (Cunningham *et al.*, 2004; Jonker *et al.*, 2007). Cetuximab has been effective in combination with other modalities in shrinking tumour masses or in delaying growth. Cetux-

imab, however, is a chimeric mAb; $\sim 34\%$ of the mAb remains murine. In fact, $\sim 19\%$ of the patients receiving cetuximab therapy have developed antibodies against cetuximab, resulting in hypersensitivity reactions and 3% of patients experienced severe reactions (Messersmith and Hidalgo, 2007)

Panitumumab, the first fully human mAb to gain FDA approval, is indicated for the treatment of patients with refractory metastatic colon cancer (Giusti *et al.*, 2007). As expected for a human mAb, panitumumab appears to be less

Table 2 Tumour and normal organ distribution of ^{111}In -panitumumab given i.v. in athymic mice bearing human tumour xenografts

Tumour	Tissue	Time of sampling after injection (h)				
		24	48	72	96	168
HT-29	Blood	7.98 ± 0.89	5.97 ± 1.71	4.48 ± 1.70	4.65 ± 0.36	2.24 ± 1.77
	Tumour	11.90 ± 3.22	19.32 ± 3.58	18.69 ± 7.26	15.88 ± 4.37	13.29 ± 6.48
	Liver	13.67 ± 1.65	13.35 ± 1.16	16.02 ± 1.60	12.08 ± 1.68	11.67 ± 1.14
	Spleen	9.16 ± 1.25	9.80 ± 3.48	10.52 ± 1.85	11.95 ± 3.69	8.63 ± 3.33
	Kidney	7.95 ± 0.55	7.00 ± 1.04	6.62 ± 0.36	5.12 ± 0.58	3.69 ± 1.10
	Lungs	4.42 ± 0.56	3.53 ± 0.61	3.53 ± 0.77	3.44 ± 0.36	1.74 ± 0.94
	Heart	2.60 ± 0.31	2.00 ± 0.25	1.98 ± 0.52	1.79 ± 0.28	1.01 ± 0.49
	Femur	1.71 ± 0.54	1.94 ± 0.22	1.86 ± 0.34	1.70 ± 0.23	1.13 ± 0.43
	LS-174T	Blood	11.69 ± 1.47	9.09 ± 0.81	6.83 ± 2.44	4.78 ± 1.98
Tumour		13.27 ± 8.40	44.08 ± 9.53	36.68 ± 20.00	29.28 ± 4.77	16.03 ± 6.40
Liver		5.76 ± 1.41	4.80 ± 2.09	4.11 ± 0.95	4.94 ± 1.95	2.83 ± 0.61
Spleen		4.28 ± 2.27	5.61 ± 1.04	5.16 ± 0.47	4.97 ± 1.33	3.45 ± 0.49
Kidney		4.81 ± 0.67	4.43 ± 0.68	3.26 ± 0.56	2.63 ± 0.42	1.67 ± 0.37
Lungs		5.44 ± 0.64	4.07 ± 0.42	3.18 ± 0.93	2.51 ± 1.03	1.55 ± 0.96
Heart		3.41 ± 0.62	2.64 ± 0.41	2.36 ± 0.66	1.72 ± 0.57	1.12 ± 0.62
Femur		1.35 ± 0.17	1.51 ± 0.17	1.23 ± 0.13	1.23 ± 0.21	0.80 ± 0.26
SHAW		Blood	10.54 ± 1.76	9.73 ± 1.05	5.79 ± 1.88	6.27 ± 2.60
	Tumour	20.50 ± 13.22	23.26 ± 11.09	28.08 ± 12.43	29.35 ± 7.40	25.57 ± 5.61
	Liver	5.21 ± 1.45	4.92 ± 1.45	4.93 ± 2.45	4.51 ± 0.39	3.45 ± 1.06
	Spleen	3.95 ± 0.98	4.49 ± 0.93	3.57 ± 0.77	3.87 ± 1.29	3.45 ± 0.72
	Kidney	3.32 ± 0.67	3.39 ± 0.40	2.28 ± 0.59	2.43 ± 0.78	1.77 ± 0.36
	Lungs	5.27 ± 2.62	4.69 ± 0.54	3.00 ± 0.84	3.15 ± 1.38	2.29 ± 0.61
	Heart	3.43 ± 0.94	3.33 ± 0.61	1.84 ± 0.55	2.34 ± 0.84	1.13 ± 0.22
	Femur	1.76 ± 1.41	1.38 ± 0.17	1.01 ± 0.33	0.93 ± 0.45	0.92 ± 0.23
	SKOV-3	Blood	11.07 ± 1.93	8.57 ± 1.81	6.95 ± 1.75	4.87 ± 1.09
Tumour		21.63 ± 18.14	24.07 ± 6.46	30.81 ± 5.44	27.50 ± 9.31	23.38 ± 4.28
Liver		6.31 ± 2.90	5.74 ± 1.01	6.50 ± 1.31	3.45 ± 0.94	3.76 ± 0.99
Spleen		6.02 ± 3.07	5.32 ± 0.71	4.71 ± 0.66	3.52 ± 0.57	3.14 ± 0.53
Kidney		4.43 ± 0.59	4.18 ± 1.17	3.11 ± 0.48	2.50 ± 0.39	1.80 ± 0.25
Lungs		5.36 ± 1.01	4.26 ± 0.86	3.56 ± 0.89	3.05 ± 0.80	1.78 ± 0.29
Heart		3.36 ± 0.52	2.65 ± 0.45	2.19 ± 0.60	1.49 ± 0.23	1.11 ± 0.23
Femur		1.49 ± 0.23	1.36 ± 0.19	1.22 ± 0.23	0.99 ± 0.19	0.81 ± 0.15

Athymic mice bearing human tumour xenografts were injected (i.v.) with ^{111}In -panitumumab (~7.5 μCi). The mice were killed by exsanguination; the tumour, blood and tissues were removed, weighed, and the radioactivity measured. The values represent the average percentage of injected dose per gram of tissue (%ID·g⁻¹) with standard deviations.

immunogenic with only 4% of the patients developing antibodies against the mAb, with 1% of the reactions being severe (Messersmith and Hidalgo, 2007). With the relative success of panitumumab in the clinic, the aim of the present study was to evaluate this mAb as a RIC compound for targeting EGFR, both *in vitro* and *in vivo*.

In order to label panitumumab with a metallic radionuclide such as ^{111}In , a bifunctional chelate is required (Wu *et al.*, 1997). The acyclic CHX-A''-DTPA chelate, which forms stable complexes with several medically relevant radionuclides, was chosen for these studies (Garmestani *et al.*, 2002; Milenic *et al.*, 2002; 2004b). Based on *in vitro* assays, modification of the antibody with 1–2 CHX-A''-DTPA molecules per antibody molecule did not affect binding to EGFR. The concentration of panitumumab-CHX-A'' required for 50% inhibition in a competition radioimmunoassay (~0.2 nM) is comparable to published data generated using BIAcore technology (Yang *et al.*, 1999). Likewise, the immunoreactivity and specificity of the immunoconjugate remained intact following labelling with ^{111}In as demonstrated by the ability of the ^{111}In -CHX-A''-panitumumab to bind A431 cells. The number of chelates-to-protein, specific activity, and immunoreactivity of the panitumumab conjugate using CHX-A''-DTPA is comparable to that reported for cetuximab (Milenic *et al.*, 2008).

In vivo targeting of A431 xenografts by ^{111}In -CHX-A''-panitumumab further validated the potential of panitumumab for imaging and/or therapeutic purposes. High tumour %ID·g⁻¹ were obtained in each of the tumour xenografts that were evaluated while the normal organs, with the exception of the blood and salivary glands, had less than 5%. Interestingly, in the absence of tumour, the pattern of radioactivity uptake is appreciably different suggesting that in the absence of an 'antigen sink', the radiolabelled panitumumab may be available to bind EGFR present in normal tissues. It is also noteworthy that the xenograft of the cell line with the highest EGFR expression did not result in the highest %ID·g⁻¹. In fact, the xenograft with the greatest uptake of ^{111}In -panitumumab was obtained with a cell line with rather low EGFR expression as measured by flow cytometry. This dichotomy, noted previously by this laboratory and others, illustrates that *in vitro* analysis of a mAb may not be predictive of *in vivo* behaviour and that the *in vivo* potential of RIC compounds should be empirically determined (Horan Hand *et al.*, 1985; Garmestani *et al.*, 2002).

Anti-EGFR antibodies have shown clinical utility in a variety of cancers such as colon, head and neck, lung, pancreas, prostate, breast, ovary, bladder, brain and renal (Baselga and Arteaga, 2005). Having demonstrated excellent

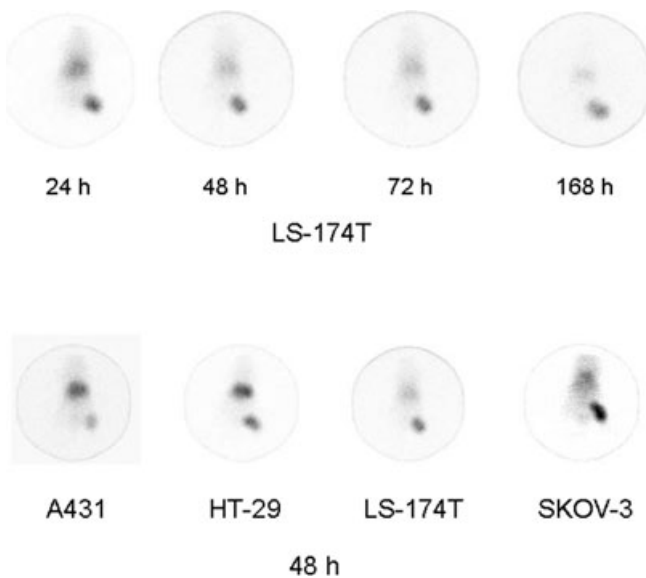


Figure 4 γ -Scintigraphy of mice bearing tumour xenografts. Following i.v. injection with 80–100 μ Ci of ^{111}In -CHX-A'-panitumumab, mice bearing LS-174T (upper row) xenografts were imaged over a 1 week period. γ -Scintigraphy was also conducted with other tumour xenograft models with representative scintigraphs taken at 48 h presented in the lower panel.

tumour targeting of the ^{111}In -panitumumab in the A431 tumour xenograft model, targeting in additional xenograft models was explored to validate its potential as a RIC in other tumours. Excellent tumour targeting was attained in four additional tumour models including the LS-174T colon carcinoma. Targeting of this latter tumour xenograft has also been demonstrated by using radiolabelled trastuzumab, cetuximab, COL-1 and CC49 (Colcher *et al.*, 1988; Milenic *et al.*, 1991; Siler *et al.*, 1993; Garmestani *et al.*, 2002; Milenic *et al.*, 2008). In this study, using the same LS-174T xenograft model, the tumour $\%ID \cdot g^{-1}$ of ^{111}In -panitumumab attained levels that are comparable to ^{111}In -labelled cetuximab and trastuzumab following i.v. injection (Garmestani *et al.*, 2002; Milenic *et al.*, 2008). The availability of different RICs that can effectively target different epitopes on the same cancer cell or tumour will allow their combined use for more efficient tumour cell killing.

The blood pharmacokinetics of ^{111}In -CHX-A'-panitumumab following i.v. injection in tumour-bearing mice was comparable to that reported for ^{111}In -labelled cetuximab (Milenic *et al.*, 2008). In the absence of tumour, however, a very different scenario was observed. The biphasic pharmacokinetic profile for panitumumab was 5.2- and 3.8-fold faster, compared with the non-tumour-bearing mice, for the $t_{1/2\alpha}$ and $t_{1/2\beta}$ phases respectively. In contrast, the pharmacokinetics of ^{111}In -cetuximab was 3.5-fold and 2.2-fold slower in the presence of tumour as compared with that in the absence of tumour. It should also be noted that while the pharmacokinetics of the two mAbs are similar in tumour-bearing mice, panitumumab has a longer elimination phase in patients than does cetuximab (7.5 vs. 5 days), thus allowing a 2-week dosing schedule for panitumumab. The possibility of circulating EGFR in the serum may provide one explanation

for the differences in the blood pharmacokinetics. Complexation of the radiolabelled antibody with EGFR in the serum would most likely result in prolonging the residence time of the ^{111}In -panitumumab in the blood. If this were true, however, one could suggest that the radiolabelled mAb would also be prevented from targeting the tumour xenografts, but our biodistribution data and γ -scintigraphy would suggest otherwise. It has already been observed that circulating antigen does not necessarily have a negative impact on tumour targeting and in fact can serve as a marker for positive selection of patients (Carrasquillo *et al.*, 1988). The influence of circulating EGFR on the *in vivo* behaviour of radiolabelled is certainly worth investigating.

Our study here shows that panitumumab can be efficiently labelled with ^{111}In by using the bifunctional acyclic CHX-A'-DTPA chelate. High specific activities can be achieved while preserving the immunoreactivity of the mAb. The studies also demonstrate tumour targeting of tumour xenografts. The chelate used for labelling can also be used for other useful metallic radionuclides such as ^{86}Y for imaging and ^{177}Lu , ^{90}Y , ^{212}Bi and ^{213}Bi for therapeutic applications. Based on this pre-clinical evaluation, it is clear that panitumumab, as a RIC, can play a positive role in future applications to cancer therapy. Studies are continuing to further evaluate the role of panitumumab in the areas of radioimmunotherapy (α - and β -emitters) and radioimmunodiagnosis (single photon emission computed tomography and positron emission tomography).

Acknowledgement

This research was supported by the Intramural Research Program of the National Institutes of Health, National Cancer Institute, Center for Cancer Research.

Conflict of interest

None.

References

- Baselga J (2002). Why the epidermal growth factor receptor? The rationale for cancer therapy. *Oncologist* 7 (Suppl. 4): 2–8.
- Baselga J, Arteaga CL (2005). Critical update and emerging trends in epidermal growth factor receptor targeting in cancer. *J Clin Oncol* 23: 2445–2459.
- Boswell CA, Eck PK, Regino CA, Bernardo M, Wong KJ, Milenic DE *et al.* (2008). Synthesis, characterization, and biological evaluation of integrin $\alpha v \beta 3$ -targeted PAMAM dendrimers. *Mol Pharm* 5: 527–539.
- Carrasquillo JA, Sugarbaker P, Colcher D, Reynolds JC, Esteban J, Bryant G *et al.* (1988). Radioimmunoscintigraphy of colon cancer with iodine-131-labeled B72.3 monoclonal antibody. *J Nucl Med* 29: 1022–1030.
- Cohenuram M, Saif MW (2007). Panitumumab the first fully human monoclonal antibody: from the bench to the clinic. *Anticancer Drugs* 18: 7–15.
- Colcher D, Minelli MF, Roselli M, Muraro R, Simpson-Milenic D,

- Schlom J (1988). Radioimmunolocalization of human carcinoma xenografts with B72.3 second generation monoclonal antibodies. *Cancer Res* **48**: 4597–4603.
- Cunningham D, Humblet Y, Siena S, Khayat D, Bleiberg H, Santoro A *et al.* (2004). Cetuximab monotherapy and cetuximab plus irinotecan in irinotecan-refractory metastatic colorectal cancer. *N Engl J Med* **351**: 337–345.
- Fraker PJ, Speck JC Jr (1978). Protein and cell membrane iodinations with a sparingly soluble chloroamide, 1,3,4,6-tetrachloro-3a,6a-diphrenylglycoluril. *Biochem Biophys Res Commun* **80**: 849–857.
- Garmestani K, Milenic DE, Plascjak PS, Brechbiel MW (2002). A new and convenient method for purification of ^{86}Y using a Sr(II) selective resin and comparison of biodistribution of ^{86}Y and ^{111}In labeled Herceptin. *Nucl Med Biol* **29**: 599–606.
- Giusti RM, Shastri KA, Cohen MH, Keegan P, Pazdur R (2007). FDA drug approval summary: panitumumab (Vectibix). *Oncologist* **12**: 577–583.
- Greiner JW (1986). Recombinant human leukocyte interferon induces alterations in the antigen phenotype of human breast carcinoma cells. *Anticancer Res* **6**: 653–658.
- Guadagni F, Witt PL, Robbins PF, Schlom J, Greiner JW (1990). Regulation of carcinoembryonic antigen expression in different human colorectal tumor cells by interferon-gamma. *Cancer Res* **50**: 6248–6255.
- Horan Hand P, Colcher D, Salomon D, Ridge J, Noguchi P, Schlom J (1985). Influence of spatial configuration of carcinoma cell populations on the expression of a tumor-associated glycoprotein. *Cancer Res* **45**: 833–840.
- Iwahashi M, Milenic DE, Padlan EA, Bei R, Schlom J, Kashmiri SV (1999). CDR substitutions of a humanized monoclonal antibody (CC49): contributions of individual CDRs to antigen binding and immunogenicity. *Mol Immunol* **36**: 1079–1091.
- Jonker DJ, O'Callaghan CJ, Karapetis CS, Zalcberg JR, Tu D, Au HJ *et al.* (2007). Cetuximab for the treatment of colorectal cancer. *N Engl J Med* **357**: 2040–2048.
- Knox SJ, Goris ML, Trisler K, Negrin R, Davis T, Liles T-M *et al.* (1996). Yttrium-90-labeled anti-CD20 monoclonal antibody therapy of recurrent B-cell lymphoma. *Clin Cancer Res* **2**: 457–470.
- Lowry OH, Rosebrough NJ, Farr AL, Randall RJ (1951). Protein measurement with the folin phenol reagent. *J Biol Chem* **193**: 265–275.
- Mendelsohn J, Baselga J (2006). Epidermal growth factor receptor targeting in cancer. *Semin Oncol* **33**: 369–385.
- Messersmith WA, Hidalgo M (2007). Panitumumab, a monoclonal anti epidermal growth factor receptor antibody in colorectal cancer: another one or the one? *Clin Cancer Res* **13**: 4664–4666.
- Milenic DE, Yokota T, Filpula DR, Finkelman MA, Dodd SW, Wood JF *et al.* (1991). Construction, binding properties, metabolism, and tumor targeting of a single-chain Fv derived from the pancarcinoma monoclonal antibody CC49. *Cancer Res* **51**: 6363–6371.
- Milenic DE, Garmestani K, Chappell LL, Dadachova E, Yordanov A, Ma D *et al.* (2002). *In vivo* comparison of macrocyclic and acyclic ligands for radiolabeling of monoclonal antibodies with ^{177}Lu for radioimmunotherapeutic applications. *Nucl Med Biol* **29**: 431–442.
- Milenic DE, Brady ED, Brechbiel MW (2004a). Antibody-targeted radiation cancer therapy. *Nat Rev Drug Discov* **3**: 488–499.
- Milenic DE, Garmestani K, Dadachova E, Chappell LL, Albert P, Hill D *et al.* (2004b). Radioimmunotherapy of human colon carcinoma xenografts using a ^{213}Bi -labeled domain-deleted humanized monoclonal antibody. *Cancer Biother Radiopharm* **19**: 135–148.
- Milenic DE, Garmestani K, Brady ED, Albert PS, Ma D, Abdulla A *et al.* (2005). Alpha-particle radioimmunotherapy of disseminated peritoneal disease using a (^{212}Pb) -labeled radioimmunoconjugate targeting HER2. *Cancer Biother Radiopharm* **20**: 557–568.
- Milenic DE, Wong KJ, Baidoo KE, Ray GL, Garmestani K, Williams M *et al.* (2008). Cetuximab: pre-clinical evaluation of a monoclonal antibody targeting EGFR for radioimmunodiagnostic and radioimmunotherapeutic applications. *Cancer Biother Radiopharm* **23**: 619–631.
- Pippin CG, Parker TA, McMurry TJ, Brechbiel MW (1992). Spectrophotometric method for the determination of a bifunctional DTPA ligand in DTPA-monoclonal antibody conjugates. *Bioconj Chem* **3**: 342–345.
- Regino CAS, Wong KJ, Milenic DE, Holmes EH, Garmestani K, Choyke PL *et al.* (2009). Preclinical evaluation of a monoclonal antibody (3C6) specific for prostate-specific membrane antigen. *Curr Radiopharm* **2**: 9–17.
- Salomon DS, Brandt R, Ciardiello F, Normanno N (1995). Epidermal growth factor-related peptides and their receptors in human malignancies. *Crit Rev Oncol Hematol* **19**: 183–232.
- Siler K, Eggensperger D, Hand PH, Milenic DE, Miller LS, Houchens DP *et al.* (1993). Therapeutic efficacy of a high-affinity anticarcinoembryonic antigen monoclonal antibody (COL-1). *Biotechnol Ther* **4**: 163–181.
- Vose JM, Wahl RL, Saleh M, Rohatiner AZ, Knox SJ, Radford JA *et al.* (2000). Multicenter phase II study of iodine-131 tositumomab for chemotherapy-relapsed/refractory low-grade and transformed low-grade B-cell non-Hodgkin's lymphomas. *J Clin Oncol* **18**: 1316–1323.
- Wells A (1999). EGF receptor. *Int J Biochem Cell Biol* **31**: 637–643.
- Wu C, Kobayashi H, Sun B, Yoo TM, Paik CH, Gansow OA *et al.* (1997). Stereochemical influence on the stability of radio-metal complexes *in vivo*. Synthesis and evaluation of the four stereoisomers of 2-(p-nitrobenzyl)-trans-CyDTPA. *Bioorg Med Chem* **5**: 1925–1934.
- Xu H, Baidoo K, Gunn AJ, Boswell CA, Milenic DE, Choyke PL *et al.* (2007). Design, synthesis, and characterization of a dual modality positron emission tomography and fluorescence imaging agent for monoclonal antibody tumor-targeted imaging. *J Med Chem* **50**: 4759–4765.
- Yang XD, Jia XC, Corvalan JR, Wang P, Davis CG, Jakobovits A (1999). Eradication of established tumors by a fully human monoclonal antibody to the epidermal growth factor receptor without concomitant chemotherapy. *Cancer Res* **59**: 1236–1243.